Pressure Recovery in Chemical Lasers

Richard J. Driscoll* and Lamar F. Moon†
Bell Aerospace Textron, Buffalo, New York

A one-dimensional flow model of the chemical laser, from combustor to subsonic diffuser, is developed for the study of laser pressure recovery. Combustor and flow chemistry effects, nozzle and cavity boundary-layer losses, laser cavity combustion, and nozzle, cavity, and diffuser geometry influences are included in the analysis. The results from experimental tests on a laser nozzle array with a constant area diffuser are presented. Diffuser exit pressures as high as 263 Torr were measured during these experiments. The one-dimensional flow model is shown to be in agreement with the measured diffuser exit pressures over the full range of test conditions.

Nomenclature

A = area
AR = nozzle area ratio
C_{pj} = jth station molar heat capcity, $\sum_i X_{ji} C_{pi}$
D_H = cavity exit hydraulic diameter
h_{fi} = ith specie heat of formation
$\hat{h}_j$ = jth station sensible enthalpy, $\sum_i \int_0^{T_j} C_{pi} dT$
h_{0_j} = jth station stagnation enthalpy, $h_j + 1/2\, M_{wj} U_j^2$
h_j = jth station enthalpy, $h_{0j} + \sum_i X_{ji} h_{fi}$
H_j = jth station total enthalpy, $n_j h_j$
m = mass flow
M = Mach number, $U/(\gamma RT)^{1/2}$
M_{wj} = jth stream molecular weight, $\sum_i X_{ji} M_{wi}$
n = molar flow
$\hat{n}_{p_{F_2}}$ = fluorine available in cavity as F_2, $1/2\, n_{pF} + n_{pF_2}$
P = pressure
Q = cavity heat release
$\hat{q}$ = normalized heat release, $Q/\hat{n}_{p_{F_2}}$
R = gas constant
R_L = cavity mixture ratio, $n_{sD_2}/\hat{n}_{p_{F_2}}$
T = temperature
U = velocity
X_{ji} = mole fraction, n_{ji}/n_j; $X_p = n_p/n_3$, $X_s = n_s/n_3$
Y_{ji} = mass fraction, m_{ji}/m_j
α_F = fluorine dissociation, $1/2\, n_{pF}/\hat{n}_{p_{F_2}}$
α_D = deuterium dissociation, n_{4D}/n_{pF}
γ = specific heat ratio
σ = laser specific power, $\mathcal{P}_\ell/m_3$
ψ_j = jth stream dilution level, $\sum_i \psi_{ji}$

$$= \sum_i (n_{ji}/\hat{n}_{p_{F_2}}),\ i \neq F, F_2$$

Subscripts

0 = stagnation state
$1-7$ = flow stations; Fig. 1
c = constant area diffuser
i = specie index (F, F_2, D, D_2, He, HF, CF_4, etc.)
I = inviscid
j = station index; at station 3: p, s, or 3 (primary, secondary, or mixed)
p = primary, oxidizer stream
s = secondary, fuel stream
T = second throat diffuser

Received June 1, 1976; revision received Feb. 4, 1977.
Index categories: Lasers; Reactive Flows; Nozzle and Channel Flows.

*Principal Scientist, High Energy Laser Technology. Member AIAA.
†Principal Scientist, Experimental Fluid Mechanics.

Introduction

PAST studies of chemical lasers have concentrated on understanding the fluid dynamic and chemical phenomena that govern power generation. A comprehensive review of this work is given by Warren.[1] Less attention has been given to the problem of pressure recovery in chemical laser flows. Efficient chemical lasers require cavity pressures in the range 5-25 Torr.[2] For open-cycle operation at sea level, some means must be found to pump the laser effluent from the low cavity pressures to 1 atm. Usually the laser cavity exit flow is supersonic; a diffuser can, therefore, be used to recover the laser flow to pressures in the 200-400 Torr range. From this level, an auxiliary pump, such as an ejector, must be used to reach 1 atm. System considerations dictate that the ejector-pumping requirements be minimized. Therefore, the attainment of high diffuser exit pressures, i.e., pressure recovery, is an important requirement for a laser system.

To date, studies of pressure recovery in chemical lasers have concentrated on the cavity flow. Warren[3] examined the laser cavity flow for constant area and constant pressure boundary conditions. Durran and Liu[4] present results for flows in which the chemical reactions occur partially at constant

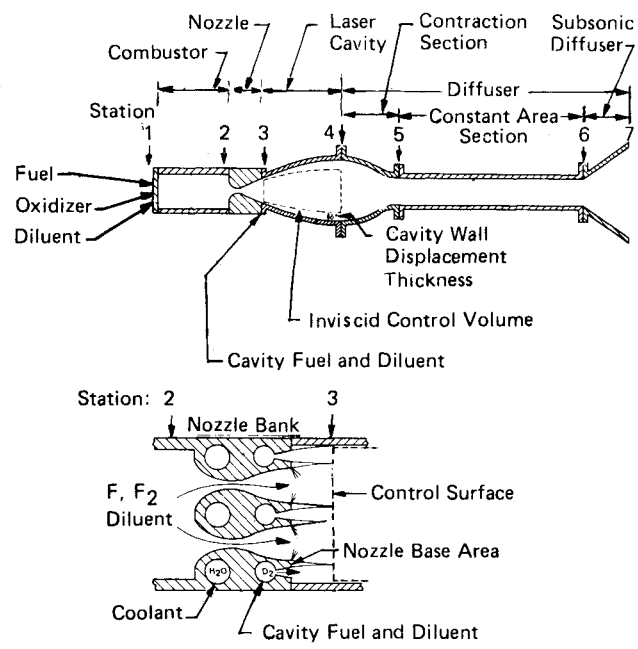

Fig. 1 Flow system and nozzle geometry.

pressure and partially at constant area; they also measured 200 Torr pitot pressures on a combustion-driven laser at the exit of a constant-area diffuser. Both studies indicate a constant-area cavity will provide better pressure recovery than will a constant-pressure cavity. Studies of supersonic combustion presented by Ferri et al.,[5,6] Billig et al.,[7-9] and Cookson et al.[10] are also applicable to the laser cavity flow. Billig[7] obtained a general solution to the one-dimensional flow equations with heat addition using a pressure-area relationship proposed by Crocco.[11] This formulation will be used herein, since it allows study of laser cavity flows in which area and pressure vary simultaneously (constant area and constant pressure flows can be obtained as special cases).

The model proposed for study is shown in Fig. 1. The influence on pressure recovery of the combustor, laser nozzles, cavity, and diffuser are considered. Flow chemistry and nozzle viscous effects are included in the analysis. A model for the flow in each component is developed and integrated to obtain the diffuser exit pressure. The results of a parametric study to identify the important variables are presented. Experimental measurements of diffuser exit pressures taken in a laser-flow experiment with a constant-area diffuser are shown. Finally, conclusions drawn from the experiment and analysis are given.

Analysis

The flow system from combustor inlet (station 1) to diffuser exit (station 7) is shown in Fig. 1. In the nozzles (stations 2-3), the flow is accelerated to supersonic velocities and low static pressures. In the laser cavity (stations 3-4), the flow is characterized by the heat release due to combustion. In the diffuser (stations 4-7), the flow is decelerated from supersonic to subsonic velocities with a corresponding increase in the gas pressure. The methods used to analyze the flow in the laser-cavity and diffuser sections will now be outlined.

Cavity Chemistry

The oxidizer (primary) flow consists of diluents, F, and F_2. The fuel (secondary) flow contains D_2 and additional diluent. If the fluorine is fully dissociated, the primary cavity chemical reaction is $F+D_2 \rightarrow DF+D$, i.e, the cold reaction; if both F and F_2 are presented, the oxidizer is consumed in the chain reaction $F+D_2 \rightarrow DF+D$, $D+F_2 \rightarrow DF+F$. The oxidizer stream variables are given the subscript p; the fuel stream variables are given the subscript s. The molar flow rates of atomic and molecular fluorine at the nozzle exit are n_{pF} and n_{pF_2}. The relative flourine dissociation is defined as $\alpha_F = 1/2\, n_{pF}/\hat{n}_{pF_2}$, where $\hat{n}_{pF_2}$ is the flow rate of all the fluorine if it were in molecular form, i.e., $\hat{n}_{pF_2} = 1/2\, n_{pF} + n_{pF_2}$; $\hat{n}_{pF_2}$ is a convenient normalization parameter for the general case where both F and F_2 are present. The molar flow rate of the primary flow species other than F and F_2 is given by the dilution level parameter $\psi_{pi} = n_{pi}/\hat{n}_{pF_2}$; the overall dilution level of the oxidizer flow is $\psi_p = \Sigma\psi_{pi}$. The molar flow rates of F and F_2 in terms of $\hat{n}_{pF_2}$ are $n_{pF} = 2\alpha_F \cdot \hat{n}_{pF_2}$ and $n_{pF_2} = (1-\alpha_F)\cdot\hat{n}_{pF_2}$, respectively. The total molar flow in the oxidizer stream is given by $n_p = \hat{n}_{pF_2}(1+\alpha_F+\psi_p)$.

The molar flow rate of the fuel stream species is also defined in terms of $\hat{n}_{pF_2}$. The deuterium flow is $n_{sD_2} = R_L \cdot \hat{n}_{pF_2}$; the secondary stream diluent flow rate is equal to $\psi_s \hat{n}_{pF_2}$. The total molar flow in the fuel stream is $n_s = \hat{n}_{pF_2}(R_L+\psi_s)$. The total cavity inlet flow, the sum of the fuel and oxidizer flows, is

$$n_3 = \hat{n}_{pF_2}(1+\alpha_F+\psi_p+\psi_s+R_L) \tag{1}$$

In the laser cavity, the diluents take no part in the chemical reactions. At the laser cavity exit, the F and F_2 are assumed to be fully reacted to DF. From an atom balance, the cavity exit DF flow rate is $n_{4DF} = 2\hat{n}_{pF_2}$. The cavity exit atomic deuterium flow rate is written $n_{4D} = \alpha_D n_{pF} = 2\alpha_F\alpha_D\hat{n}_{pF_2}$ where α_D is defined as the D atom dissociation parameter; when $\alpha_D = 1$, no recombination has occurred; when $\alpha_D = 0$, the deuterium is fully recombined. The molecular deuterium flow rate at the cavity exit is $n_{4D_2} = \hat{n}_{pF_2}(R_L - 1 - \alpha_F\alpha_D)$, and the total molar flow rate at the cavity exit is given by Eq. (2). When $\alpha_D = 1$, $n_4 = n_3$, and the cavity flow is equimolar.

$$n_4 = \hat{n}_{pF_2}(1+\alpha_F\alpha_D+\psi_p+\psi_s+R_L) \tag{2}$$

Cavity Thermochemistry

The enthalpy of the cavity inlet and exit flow is $H_3 = n_3h_3$ and $H_4 = n_4h_4$. If laser cavity flow were adiabatic, then H_3 would equal H_4. Energy, however, is removed from the cavity in the form of laser power; convective heat transfer through the cavity walls is neglected. The laser power extracted is written in terms of the specific power (power extracted/mass flow), as $\mathcal{P}_\ell = n_3 M_{w3}\sigma$. The energy equation is then written as $H_3 = H_4 + \mathcal{P}_\ell$.

Substituting the expressions for n_3, n_4, h_3, and h_4 into those for H_3 and H_4, the energy equation can be written

$$(n_4h_{04} - n_3h_{03}) + n_3M_{w3}\sigma = Q = \sum_i (n_{3i}h_{fi} - n_{4i}h_{fi}) \tag{3}$$

The left-hand side represents the energy that heats the gas and is extracted as laser power; the right-hand side is the heat released by the chemical reactions, i.e., Q. Of those species that enter the laser cavity at station 3, only F, F_2, and D_2 take part in the cavity reactions; the corresponding products at the cavity exit are DF and D. Complete reaction of the fluorine in the cavity is assumed. For the diluent species, $n_{3i} = n_{4i}$; for F_2 and D_2, the standard state heat of formation is zero. Therefore, Q can be written

$$Q = n_{pF}h_{fF} - n_{4DF}h_{fDF} - n_{4D}h_{fD} \tag{4}$$

Using the relationships for the F, DF, and D flow rates given previously, the cavity heat release can be written in terms of $\hat{n}_{pF_2}$, α_F, and α_D

$$\hat{q} = Q/\hat{n}_{pF_2} = 2\alpha_F(h_{fF} - \alpha_D h_{fD}) - 2h_{fDF} \tag{5}$$

For the cold-reaction chemical laser, i.e., $\alpha_F = 0(1)$, $\hat{q}$ equals 69 kcal/mole when $\alpha_D = 1$ and is equal to 173 kcal/mole when $\alpha_D = 0$. For the chain-reaction laser, i.e., $\alpha_F = 0(0.1)$, $q \cong 125$ kcal/mole and is essentially independent of α_D. Since three-body recombination processes are generally slow in the laser cavity due to the low static pressure, deuterium atom recombination will be negligible in the laser cavity. Therefore, α_D will be 0(1) at the cavity exit and for the cold-reaction laser, energy will leave the cavity in the form of chemical potential energy, i.e., dissociated deuterium. With $\alpha_D = 1$, at chain reaction conditions $\hat{q}$ is approximately twice as large as that for the cold reaction laser, i.e., 125 vs 69 kcal/mole.

With $\alpha_D = 1$, the cavity flow is equimolar; therefore, $n_4 = n_3$ and $M_{w3} = M_{w4}$. Using Eqs. (1), (2), and (3), the stagnation enthalpy ratio across the laser cavity can be written

$$\frac{h_{04}}{h_{03}} = 1 + \frac{1}{\lambda}\left[\frac{\hat{q}/h_{0p}}{1+\alpha_F+\psi_p} - \frac{M_{w3}\sigma}{X_p h_{0p}}\right] \tag{6}$$

The parameter h_{0p} is the primary nozzle exit stagnation enthalpy and is reduced from h_{02} by the nozzle heat loss, e.g., if the nozzle flow were adiabatic, $h_{0p} = h_{02}$; λ describes this influence of the secondary stream on h_{04}/h_{03}

$$\lambda = 1 + \frac{X_s h_{0s}}{X_p h_{0p}} \tag{7}$$

Fluid Dynamics

A one-dimensional flow model is used for the laser cavity and diffuser analyses. This implies that the transverse

velocities are small compared to the axial velocity at the control surfaces for which the conservation equations are written. Furthermore, the equations are written in terms of uniform flow parameters at each control surface. The degree to which these assumptions are valid at the control surfaces used in this analysis will now be examined.

The flow conditions at the exits of the fuel and oxidizer nozzles are obtained from the combustor and nozzle analyses; the nozzle exit flowfields are nonuniform due to the nozzle boundary layer. The flow properties, e.g., velocity, pressure, Mach number, etc., of the fuel and oxidizer nozzles are generally not the same. Uniform flow parameters for the nozzle exit flows are obtained by integrating the nonuniform distributions across the nozzles using the method given in Ref. 12. Also, since laser nozzles are usually either contoured or have small divergence angles, their transverse velocities are small and the flow can be considered as one-dimensional. The flow through a control surface placed at the nozzle exit plane can, therefore, be described as one-dimensional and piecewise uniform, as long as the nozzle flows are not separated. Between the two nozzles is a small base area. It is assumed that the interaction between the two nozzle flows and the cavity wall results in a base pressure that does not result in separated nozzles flows. This constraint requires that the pressure mismatch of the two nozzle flows be limited; the allowable mismatch, however, is not known.

The flowfields at the laser-cavity exit (station 4) and the constant-area diffuser inlet (station 5) are, in general, three-dimensional and nonuniform. Within the laser cavity, three-dimensional velocity/pressure fields and flow nonuniformities are generated by the cavity chemical reactions, the contoured cavity/diffuser walls, and the wall boundary layers. The rate at which these effects are produced and decay depends on the cavity mixing rates, and since laser nozzles are designed to promote rapid mixing, these effects are expected to be important in the near-nozzle region of the cavity where the heat release rate is large and small at the cavity exit and downstream locations where the chemical reactions are essentially complete. Also, the contours used for the laser cavity and diffuser walls are usually smooth large radii of curvature contours designed to duct the flow without producing large pressure gradients that would promote boundary-layer separation. The transverse velocities associated with such contours are typically small compared to the cavity axial velocity, and deviations from one-dimensional flow induced by the contoured walls can also be considered second order. Thus, for the inviscid cavity flow, while three-dimensional and nonuniform flow effects will be present at the cavity exit and downstream locations, they are expected to be of second order. As a result, the one-dimensional uniform flow equations can be expected to yield reasonably accurate characteristic values for the average inviscid flow parameters at the cavity exit and diffuser inlet.

The last control surface considered is at the constant-area diffuser exit (station 6). Assuming the constant-area diffuser is of sufficient length to contain the shock structure required to complete the supersonic to subsonic flow transition, then there is sufficient length for the mixing and dissipation processes that occur in the diffuser to eliminate any nonuniformities or three-dimensional effects at the diffuser inlet. Thus, the flowfield at this location will be essentially one-dimensional and uniform.

Cavity Inviscid Flow

The cavity control volume extends between stations 3 and 4. The flow at the inlet control surface is written as one-dimensional and piecewise uniform and at the exit as one-dimensional and uniform. The axial momentum equation is then given as

$$[PA(1+\gamma M^2)]_{4I}=\sum_{k=1}^{3}[(PA(1+\gamma M^2)]_3+\int_3^4 P\cdot dA$$

where the k index at station 3 refers to the three regions at this control surface, i.e., the fuel and oxidizer nozzle flows and the base area. The subscript I at station 4 indicates the cavity flow is inviscid; the exit flow area A_{4I} is less than the geometric flow area A_4 by A_{δ^*}, the area displaced by the cavity boundary layers. Except for the limiting cases of constant-area or constant-pressure cavity flows, this equation is difficult to use to obtain simple closed-form solutions for the cavity-exit flow parameters, particularly since the pressure under the integral is not uniform at the cavity inlet. A simplification is therefore introduced. The mixing and reaction processes that occur simultaneously in the cavity are separated into two discrete steps: the cavity inlet flow is allowed to mix and fill the cavity inlet area, producing a uniform flowfield; the cavity exit flow is then obtained by determining the response of the uniform cavity inlet flow to the heat release. It is shown in the Appendix that, for a constant-area cavity, the cavity exit Mach number calculated from the two-step process is the same as that obtained if mixing and heating occur simultaneously; for a constant-pressure cavity, the error associated with the two-step process is small for laser flows. In the region bounded by the constant-area and constant-pressure processes, the errors associated with the two-step process are assumed to be of the same order as those for the limiting cases. Using this approximation, then, the axial momentum equation can be written as

$$[PA(1+\gamma M^2)]_{4I}=[PA(1+\gamma M^2)]_3+\int_3^4 P\cdot dA \tag{8}$$

The uniform cavity inlet flow parameters are derived by allowing the fuel and oxidizer nozzle flows to mix without reaction while filling the nozzle base area. The nozzle base pressure is assumed equal to P_3, the mixed-flow cavity inlet pressure, since no data is available to define the actual base pressure. The value assumed for the base pressure has little effect on the calculation if P_3 is of the same order as the nozzle-exit pressures since the base-pressure term is small compared to the primary and secondary nozzle-momentum terms. With this assumption, the momentum equation solved for U_3 is

$$U_3=Y_pU_p+Y_sU_s+1/m_3[P_pA_p+P_sA_s-P_3(A_p+A_3)] \tag{9}$$

The energy equation solved for the mixed flow static enthalpy $\hat{h}_3$ is

$$\hat{h}_3=X_p\hat{h}_p+X_s\hat{h}_s+1/2M_{ws}[Y_pU_p^2+Y_sU_s^2-U_3^2] \tag{10}$$

and the continuity equation solved for P_3 is

$$P_3=\frac{m_3R_3T_3}{U_3A_3} \tag{11}$$

These three equations are solved by iteration, using temperature-dependent gas properties, to obtain P_3, U_3, and T_3; the remaining parameters, such as P_{03} and M_3 are then computed.

Having defined flow properties at station 3 suitable for use in Eq. (8), it now remains to evaluate the pressure integral. For constant-area flows, the pressure integral is zero, whereas for constant-pressure flows, the pressure integral is $P_3\ (A_4-A_3)$; for the general case where $P=f(A)$, it is necessary to know the pressure/area relationship in order to evaluate the integral. Herein, the method devised by Crocco[11] will be used. The pressure/area relationship is

$$P\cdot A^{\epsilon/(\epsilon-1)}=\text{constant} \tag{12}$$

Constant-area cavity flow is given by $\epsilon=1$ and constant-pressure cavity flow by $\epsilon=0$; varying ϵ in the range of $0\leq\epsilon\leq 1$ gives the solution between these limits. If Eq. (12) is

substituted into Eq. (8) to evaluate the pressure integral, the cavity static pressure and area ratios can be written in terms of the control volume inlet and exit Mach numbers

$$\frac{P_{4I}}{P_3}=\left[\frac{\epsilon+\gamma M_3^2}{\epsilon+\gamma M_{4I}^2}\right]^{\epsilon} \tag{13}$$

$$\frac{A_{4I}}{A_3}=\left[\frac{\epsilon+\gamma M_3^2}{\epsilon+\gamma M_{4I}^2}\right]^{1-\epsilon} \tag{14}$$

The cavity static temperature ratio is obtained from the perfect gas law, the continuity equation, and the defining equation for the Mach number

$$\frac{T_{4I}}{T_4}=\left[\frac{M_{4I}(\epsilon+\gamma M_3^2)}{M_3(\epsilon+\gamma M_{4I}^2)}\right]^2 \tag{15}$$

Using the isentropic relationship for flows with a constant specific heat ratio to relate P_{04I} to P_{4I} and P_{03} to P_3, the cavity stagnation pressure ratio can be written as

$$\frac{P_{04}}{P_{03}}=\frac{P_{4I}}{P_3}\left[\frac{1+\frac{\gamma-1}{2}M_{4I}^2}{1+\frac{\gamma-1}{2}M_3^2}\right]^{\frac{\gamma}{\gamma-1}} \tag{16}$$

To evaluate the preceding equations, M_{4I} must be known from previous evaluation of the energy equation. At the cavity exit, T_{04} and T_{4I} are related

$$T_{04}=T_{4I}\left(1+\frac{\gamma-1}{2}M_{4I}^2\right) \tag{17}$$

a similar equation can be written for the cavity inlet flow relating to T_{03}, T_3, and M_3. The cavity stagnation temperature ratio is then obtained by dividing T_{04} by T_{03}, and substituting Eq. (15) for T_{4I}/T_3; the result is

$$\frac{T_{04}}{T_{03}}=\left[\frac{1+\frac{\gamma-1}{2}M_{4I}^2}{1+\frac{\gamma-1}{2}M_3^2}\right]\left[\frac{M_{4I}(\epsilon+\gamma M_3^2)}{M_3(\epsilon+\gamma M_{4I}^2)}\right] \tag{18}$$

The ratio T_{04}/T_{03} is obtained by evaluating Eqs. (6) and (7); ϵ is assigned a value and Eq. (18) is then solved for M_{4I}. Once M_{4I} is known, Eqs. (13-16) can be solved for P_{4I}/P_3, A_{4I}/A_3, etc. The set of solutions between constant area and constant pressure is obtained by repeating this process varying ϵ in the range of $1\leq\epsilon\leq 0$. Note that the cavity-area ratio is obtained from Eq. (14) as part of the solution; it is not known *a priori*. Also, due to the large static temperature rise that occurs across the laser cavity γ cannot be assumed constant at the cavity inlet value; for this study, the average of the cavity inlet and exit value was used for each value of ϵ.

If the equation for the entropy increase due to heat addition is written, it is found that for any given values of ϵ, M_3, and γ, there is a maximum stagnation temperature ratio (T_{04}/T_{03}) which can be achieved. Increasing T_{04}/T_{03} above the critical value results in an entropy decrease, which is forbidden. When the critical value is reached, the flow is said to be "choked" since any further heat addition requires a change in the initial conditions. The critical Mach number at the cavity exit is given by

$$M_4^*=\left[\frac{\epsilon}{\epsilon-\gamma(\epsilon-1)}\right]^{1/2} \tag{19}$$

the critical value of T_{04}/T_{03} is obtained by substituting M_4^* for M_{4I} in Eq. (18). When $\epsilon=1$, i.e., constant area flow, $M_4^*=1.00$; when $\epsilon<1$, $M_4^*<1$. For constant pressure flows, i.e., $\epsilon=0$, $M_4^*=0$, indicating that choking occurs only in the limit of infinitely large heat addition.

Cavity Boundary Layers

At the low cavity pressures, i.e., Reynolds numbers, that characterize chemical laser flows, the cavity wall boundary layers can become large. When the boundary layers remain attached, they reduce the flow momentum available for recovery in the diffuser, change the effective contour of the cavity walls, and reduce the area available to the flow. If the cavity wall pressure gradient becomes sufficiently large, the boundary layer will separate from the wall with an attendant reduction in the area available to the flow. This can result in flow choking at the cavity exit, producing high cavity pressures and poor laser performance.

For this study, it was desirable to include cavity boundary-layer effects in the analysis to examine their influence on the cavity-exit flowfield. Boundary-layer calculations were made and the results correlated in terms of the cavity pressure ratio (P_{4I}/P_3), wall temperature, and Reynolds number; due to the low Reynolds numbers, only laminar boundary layers were considered. A linear pressure gradient over a 4-in.-long cavity was assumed; the initial boundary-layer thickness was set at 0.020 in. for all calculations. The analysis indicated that flow separation was probable when the cavity walls were adiabatic and the pressure ratio was 4-5; cooled cavity walls were found to delay separation. For the calculations presented, the cavity wall was assumed to be cooled and the boundary layers to be attached. It should be noted that the pressure field in the laser cavity is three-dimensional, and for detailed design studies, it is inadequate to perform the boundary-layer calculations using one-dimensional parameters. For design purposes, a method such as that given by Zelazny and Rushmore,[13] which includes the influence of the nonuniform pressure field, cavity contour, and reaction kinetics should be used.

The results from the boundary-layer calculations just discussed are included in the pressure recovery analysis in the following manner. The wall boundary-layer displacement (δ^*) and momentum (θ) thicknesses at the cavity exit are assumed to be known and have a uniform value on the cavity side, top, and bottom walls. The displacement area, A_{δ^*}, is then δ^* times the cavity exit perimeter, and can be written in terms of the cavity exit geometric flow area and hydraulic diameter.

$$A_{\delta^*}/A_4=4(\delta^*/D_H) \tag{20}$$

The inviscid and geometric flow areas are related by $A_4=A_{4I}+A_{\delta^*}$. The correction factors used in Ref. 12, i.e., α_1, α_2, and α_3, can be written

$$\alpha_1=1-4\frac{\delta^*}{D_H},\quad \alpha_2=1-\frac{4}{\alpha_1}\frac{\theta}{D_H},\quad \alpha_3=1 \tag{21}$$

$\alpha_3=1$ since convective heat transfer in the cavity is neglected. Having defined the correction factors, Eqs. (12)-(23) of Ref. 12 can be used to relate the inviscid flow parameters, U_{4I}, M_{4I}, T_{4I}, P_{04I}, etc. to the average cavity-exit flow parameters corrected for the boundary layer, i.e., U_4, M_4, T_4, P_{04}, etc.

Diffuser

Both constant-area and second-throat diffusers are considered. In a constant-area diffuser, no contraction is employed, i.e., $A_5/A_4=1$, and $M_5=M_4$, $P_5=P_4$, etc. For this diffuser geometry, Neuman and Lustwerk[14] have shown experimentally that, whereas the supersonic to subsonic flow transition occurs over a finite distance of 8-13 diffuser inlet hydraulic diameters through a complex mechanism involving oblique and lambda shocks and separated flow, the static pressure rise that accompanies the transition is essentially what would occur if transition occurred through a normal

shock. Therefore, the flow conditions at station 6 are computed from those at station 5 using the standard normal shock equations, e.g., Ref. 15.

Rundstandler et al.[16] have experimentally measured the performance of subsonic diffusers and described their performance in terms of a static pressure recovery coefficient η, which is a function of a number of geometric parameters including the diffuser aspect ratio, and area ratio, and wall divergence. Using Rundstandler's definition, the subsonic diffuser static pressure ratio can be written

$$\frac{P_7}{P_6} = 1 + \eta \left[\frac{P_{06}}{P_6} - 1 \right] \tag{22}$$

P_{07} is assumed equal to P_7 since $M_7 = O(0.1)$. A representative value of η is 0.50.

Experiments conducted by Hasel and Sinclair,[17] Neuman and Lustwerk,[18] and Pansesci and German[19] have demonstrated that constant-area diffuser performance can be improved upon by using a second throat diffuser such as that shown in Fig. 1. In such a diffuser, a contraction section (station 4-5) is employed to compress the flow to a higher static pressure and lower Mach number before it enters the constant-area section. The Mach number that then characterizes the normal shock process is lower than that for the corresponding constant-area diffuser; the stagnation pressure losses are therefore smaller and the diffuser static pressure ratio P_7/P_4 is greater. The minimum contraction ratio that can be employed in a fixed geometry self-starting system has been established experimentally, and is shown in Fig. 2 as a function of the diffuser inlet Mach number M_4. Aslo shown in Fig. 2 is the improvement in the diffuser exit pressure obtainable with a second throat diffuser when compared to a constant-area diffuser with the same inlet flow. Second throat diffuser performance was calculated by assuming an isentropic compression between stations 4 and 5, with the contraction ratio at the limiting value, followed by a normal shock at M_5; constant-area diffuser performance was obtained by assuming a normal shock at M_4. In practice, it is expected that the experimental results would show lower performance than indicated by the theory, since the compression between stations 4 and 5 cannot be accomplished isentropically; in this sense, the results of Fig. 2 establish an upper limit on the obtainable performance improvement.

Parametric Study

A parametric study was conducted for a DF laser to illustrate the pressure recovery performance trends of this device. A two-dimensional "trip flow" nozzle array, similar to that described by Wilson and Hook,[20] was chosen for study due to its demonstrated ability to maintain efficient laser performance at the elevated laser cavity pressures (10-20 Torr) required for high pressure recovery levels. The oxidizer

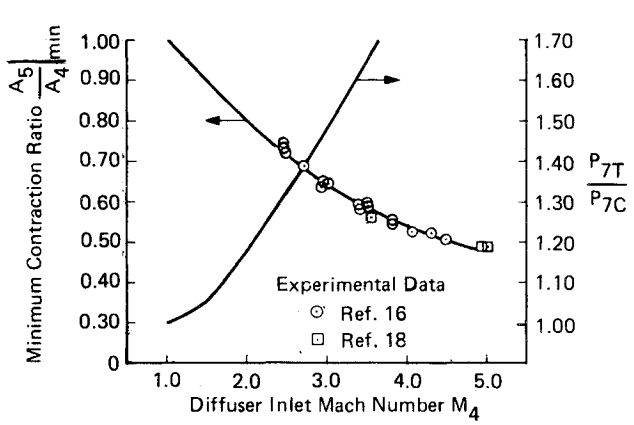

Fig. 2 Second-throat-diffuser parameters.

Table 1 Analysis parameters

	Nominal	Range
Primary flow		
Pressure, P_{0p} (atm)	15	5-20
Temperature, T_{02} (K)	1700	1100-2100
Dilution level, ψ_p	25	10-50
Secondary flow		
Temperature, T_{0s}(K)	300	300-1500
Cavity mixture ratio, R_L	5	5-15
Dilution level, ψ_s	5	0-15
Laser cavity		
Area ratio, A_4/A_3	1.60	1.00-5.00
Wall temperature, T_w/T_{03}	0.30	0.30-1.00
Diffuser		
Contraction ratio, A_5/A_4	1.00	1.00-Limit
Subsonic diffuser efficiency, η	0.50	0.00-1.00

(primary) nozzles had throat and exit widths of 0.0026 and 0.0650 in., respectively, resulting in a geometric area ratio (AR_p) of 25; the cavity fuel secondary) nozzles had throat and exit widths of 0.0030 and 0.0180 in., respectively, yielding a geometric area ratio (AR_s) of 6. There were 32 primary and 33 secondary nozzles in a nozzle array whose nominal envelope dimensions were 1×4 in.; this arrangement results in an array with 33% base area, i.e., $A_b/A_3 = 0.330$.

A listing of the variables considered in this study, with their nominal values and ranges is given in Table 1. Combustor reactants were ethylene (C_2H_4) and fluorine (F_2), with helium diluent and deuterium cavity fuel. At the nominal combustion conditions, i.e., $T_{02} = 1700$ K, $\psi_p = 25$, the fluorine is approximately fully dissociated with $\alpha_F > 0.90$; α_F is calculated from an equilibrium relationship of the form: $\alpha_F = \alpha_F\ (P_{02}, T_{02}, \psi_p)$. At the nominal secondary flow rate with $R_L = \psi_s = 5$, the primary and secondary nozzle exit pressures are equal. Mismatched pressures do occur within the range of variables considered; however, the pressure mismatch is less than a factor of two. For the nozzle design described, approximately 85% of the mass enters the laser cavity through the primary nozzles at the nominal conditions; additionally, the stagnation pressure of the secondary stream is low (~ 1 atm) compared to the primary. Therefore, the primary flow variables are expected to have a greater influence on pressure recovery than the secondary flow parameters. For the results presented in this section, it was assumed that no laser power was extracted from the laser cavity, i.e., $\sigma = 0$, in Eq. (6). Also, the numerical results presented are valid only for the nozzle design described; the performance trends, however, are generally true for this type of laser.

The cavity inlet mixed flow static pressure (P_3) and Mach number (M_3), cavity-exit Mach number (M_4), constant-area diffuser exit pressure (P_{7C}), and second-throat-diffuser exit pressure (P_{7T}) are shown in Fig. 3 as a function of combustor pressure; all other variables have their nominal values (see Table 1). The cavity-inlet pressure (P_3) varies almost linearly with combustor pressure; in the range of $P_{02} = 5$-20 atm, the cavity-inlet pressure is low and in the range of $P_3 = 6$-18 Torr. As P_{02} is reduced, the viscous losses in the laser nozzles increase, resulting in a decrease in the cavity-inlet and exit Mach numbers, M_3 and M_4; if the laser nozzle and cavity flow were inviscid, M_3 and M_4 would be independent of P_{02}. At the nominal 15 atm combustor pressure with $P_3 = 14.4$ Torr, $M_3 = 3.70$ and $M_4 = 2.27$; the constant-area and second-throat-diffuser exit pressure are $P_{7C} = 204$ Torr and $P_{7T} = 252$ Torr, respectively; for this case, the second throat diffuser yields a 25% improvement. At $P_{02} = 5$ atm, viscous effects have reduced the cavity exit Mach number to $M_4 = 2.04$; for this case, $P_{7C} = 75$ Torr, with the reduced value of M_4 resulting in only a 15% improvement for the second-throat-diffuser configuration. Note that both P_{7C} and P_{7T} are approximately linear functions of P_{02} over the range considered.

It is of interest to examine the stagnation pressure losses between the combustor and diffuser exit. With the com-

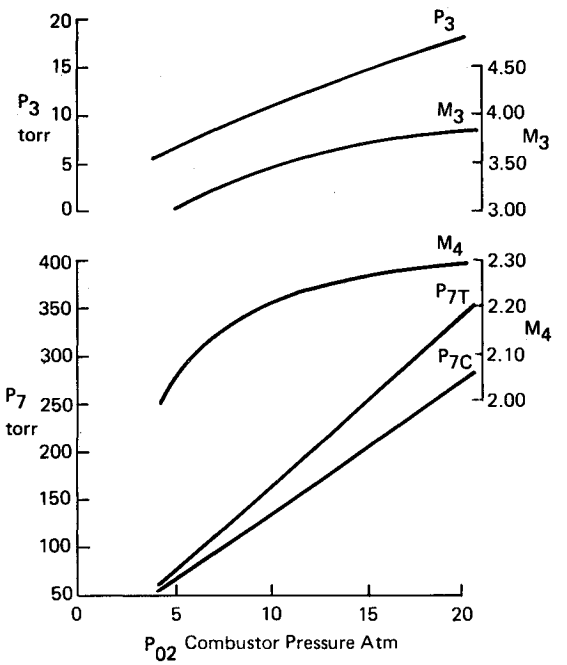

Fig. 3 Pressure recovery vs combustor pressure.

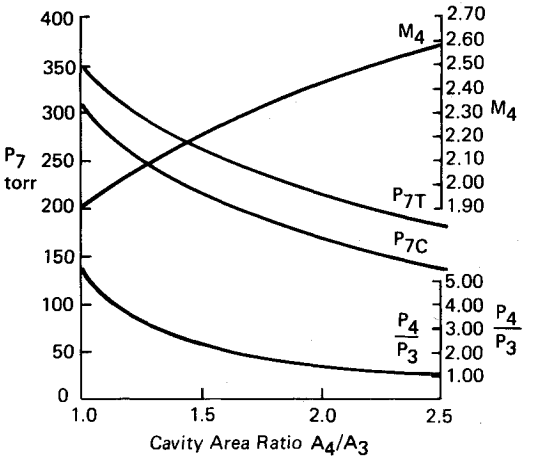

Fig. 4 Pressure recovery vs cavity-area ratio.

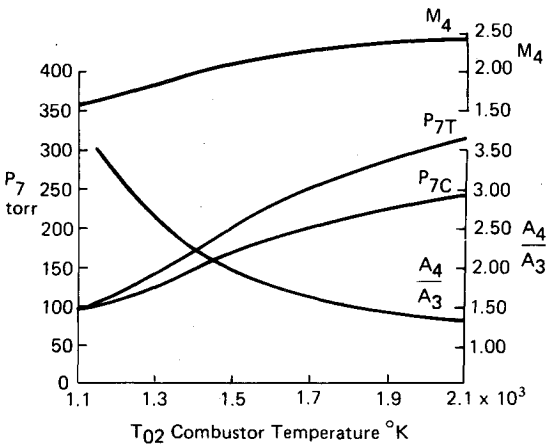

Fig. 5 Pressure recovery vs combustor temperature ($P_4/P_3 = 2.10$).

bustors as the starting point, for the nominal 15 atm case, $P_{02} = 11{,}400$ Torr. At the cavity inlet, for the mixed flow before reaction, $P_{03} = 2150$ Torr, i.e., $P_{03}/P_{02} = 0.190$, or 81% of the available stagnation pressure is lost due to the nozzle viscous losses and in mixing the low stagnation pressure secondary flow with the primary. At the cavity exit, $P_{04} = 368$ Torr, i.e., $P_{04}/P_{03} = 0.170$; 83% of the stagnation pressure available at the cavity inlets is lost due to the cavity combustion. Note that P_{04} represents the stagnation pressure available for recovery in the diffuser, and with the nozzle and cavity combustion losses, $P_{04} = 368$ Torr represents only 3.23% of the combustor pressure. For the constant-area diffuser configuration, $P_{06} = 234$ Torr, with the losses in the constant-area section due to the shock and mixing processes. A 50% efficient subsonic diffuser results in $P_{7C} = 204$ Torr. Note that the diffuser recovers approximately 55% of the stagnation pressure available at its inlet, i.e., $P_{7C}/P_{04} = 0.554$, but that the overall system pressure recovery efficiency as measured by the ratio P_{7C}/P_{02} is low, on the order of only 1.80%, due to the large stagnation pressure losses in the laser nozzles and cavity. This indicates that obtaining high levels of pressure recovery may be more a matter of controlling the nozzle and cavity stagnation pressure than of optimizing diffuser designs, e.g., for the second-throat-diffuser configuration with $P_{7T} = 252$ Torr, the overall efficiency as measured by P_{7T}/P_{02} is still only 2.21%, and for a perfectly efficient diffuser, it would be only 3.23%.

Another parameter often used to measure laser recovery is the diffuser exit/cavity inlet static pressure ratio, i.e., P_7/P_3; this parameter is useful since it can be used to relate laser performance and pressure recovery, as laser efficiency is critically dependent on the cavity static pressure. With $P_{02} = 15$ atm, and for the constant area diffuser, $P_{7C}/P_3 = 14.2$; for the second throat diffuser, $P_{7T}/P_3 = 17.5$. For this case, the cavity static pressure ratio is $P_4/P_3 = 2.10$ so that the static pressure ratio across the diffuser is on the order of 7-9. At the lower combustor pressure, $P_{02} = 5$ atm, $P_{7C}/P_3 = 10.8$, and $P_{7T}/P_3 = 12.5$, indicating that the static pressure ratios P_{7C}/P_3 and P_{7T}/P_3 are functions of the combustor pressure. The ratios P_{7C}/P_{02} and P_{7T}/P_{02} are also functions of P_{02}, and this limits the usefulness of such parameters in defining pressure recovery performance.

The change in diffuser exit pressure with the cavity area ratio (A_4/A_3) is shown in Fig. 4. In the constant pressure flow ($P_4/P_3 = 1$), the cavity exit Mach number (M_4) has its highest value, and the diffuser exit pressure (P_7) is lowest. P_7 is low since the stagnation pressure losses associated with constant pressure combustion are larger than those in a more confined flow; also the higher value of M_4 results in a larger stagnation pressure loss in the diffuser. As the cavity area ratio is decreased, M_4 decreases, reducing the diffuser stagnation pressure loss. The cavity stagnation pressure loss also decreases as A_4/A_3 is reduced. The combination of smaller cavity and diffuser losses, therefore, results in the rapid increase in the diffuser exit pressure as the cavity area ratio is reduced. Note, however, that the cavity pressure ratio increases, indicating an increasing potential for boundary-layer separation on the cavity wall.

For the nominal conditions considered herein, the cavity wall boundary layers were found to have only a second-order influence on the cavity-exit flowfield and the diffuser exit pressure. The boundary-layer influence was found to be more important at the lower cavity pressures and could have a first-order influence at cavity pressure on the order of 1 Torr.

The subsonic diffuser was assumed to operate nominally at 50% efficiency, i.e., $\eta = 0.50$ in Eq. (22); this result in $P_{7C} = 204$ Torr. With the range of $0 \le \eta \le 1$, the diffuser exit pressure can vary in the range of $174 \le P_{7C} \le 234$ Torr, i.e., a 60 Torr range. Using $\eta = 0.50$ as a baseline, and $\eta = 0.75$ as the performance of an advanced diffuser, the recovered pressure would increase by about 7% by using an advanced subsonic diffuser.

Cavity and diffuser parameters vary with T_{02} as shown in Fig. 5; for this case, the cavity is defined by $P_4/P_3 = 2.10$ and A_4/A_3 is a dependent variable. The cavity area ratio, A_4/A_3, decreases with increasing T_{02} in order to maintain $P_4/P_3 = 2.10$. As T_{02} is increased, the stagnation pressure loss in the laser cavity decreases for two reasons: first, the heat

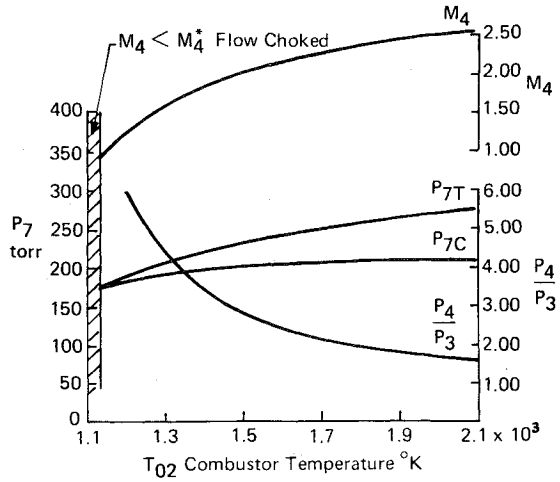

Fig. 6 Pressure recovery vs combustor temperature ($A_4/A_3 = 1.60$).

release as measured by T_{04}/T_{03} is lower, and second, the flow is more confined, i.e., A_4/A_3 is lower. The stagnation pressure loss in the diffuser increases, since the diffuser inlet Mach number increases with increasing T_{02}. As shown in Fig. 5, the diffuser exit pressure for both constant area (P_{7C}) and second throat (P_{7T}) diffusers increase with T_{02}, the reason being that the reduced cavity stagnation pressure loss outweighs the increase in the diffuser loss. In the range of interest for the cold reaction ($\alpha_F \approx 1$) chemical laser, increasing T_{02} from 1700 to 2100 K, increases P_{7C} by about 20%, from 204 to 244 Torr, and P_{7T} by about 26%, from 250 to 314 Torr. The improvement is larger for the second throat diffuser since it can take greater advantage of the increased diffuser inlet Mach number.

With the laser cavity-area ratio held constant at $A_4/A_3 = 1.60$, the cavity and diffuser parameters vary with T_{02} as shown in Fig. 6. Note the cavity exit flow chokes for $T_{02} = 1130$K, and operation in the range of $T_{02} \leq 1130$K could result in shock waves and above design pressures in the laser cavity. Flow choking can be alleviated by increasing the cavity-area ratio, flow dilution level, or combustor temperature. With A_4/A_3 held constant, the cavity pressure ratio (P_4/P_3) is now a function of T_{02}, increasing above its nominal value of 2.10 at temperatures lower than 1700K, and decreasing below 2.10 at temperatures above 1700K. As T_{02} is decreased, the cavity pressure ratio increases rapidly, indicating that flow choking could possibly occur due to cavity wall boundary-layer separation before it would occur due to purely thermal effects. P_{7C} is relatively constant at about 204 Torr for this case. The invariance of P_{7C} is due to the fact that with A_4/A_3 held constant, as T_{02} is increased, the reduction in the cavity stagnation pressure loss is just balanced by the increased diffuser loss. P_{7T} increases with increasing T_{02} due to the higher diffuser inlet Mach number, however, less rapidly than before, e.g., increasing T_{02} from 1700K to 2100K, increases P_{7T} by 10% (from 250 to 275 Torr).

The primary flow dilution level ψ_p is a measure of the inert to reactant species flow rates through the cavity. Increasing ψ_p corresponds to reducing the percentage of reactant fluorine in the flow, and thereby, the enthalpy increase per mole of cavity flow due to cavity combustion. As with T_{02}, ψ_p affects the cavity flow and pressure recovery through its influence on T_{04}/T_{03}, e.g., see Eq. (6). The trends observed by increasing ψ_p are the same as those previously shown for increasing T_{02}. For the nominal conditions, and for the laser cavity defined by $P_4/P_3 = 2.10$, increasing ψ_p from 25 to 40 increased P_{7C} by about 15%, from 204 to 235 Torr, and P_{7T} by 26%, from 250 to 315 Torr. For a fixed area ratio cavity with $A_4/A_3 = 1.60$, P_{7C} was essentially invariant at 204 Torr while P_{7T} increased by about 11%, from 250 to 277 Torr when ψ_p was increased from 25 to 40. Conversely, if ψ_p is decreased below 25, the diffuser exit pressures will decrease.

The results presented indicate that the diffuser exit pressure is relatively insensitive to T_{02} and ψ_p when the cavity area ratio A_4/A_3 is held constant, e.g., see Fig. 6; this trend has been observed experimentally and will be illustrated in the next section. These results should not be taken to indicate that there is no potential for increasing pressure recovery by increasing ψ_p and T_{02}, since large increases can be achieved when the cavity-area ratio is allowed to vary, e.g., see Fig. 5. Rather, they imply that the cavity-area ratio must be matched to each specific flow condition, and that in experiments to measure laser pressure recovery, the cavity area ratio should be considered as a primary variable.

The secondary flow parameters (T_{0s}, R_L, ψ_s) were varied over a limited range to examine their influence on pressure recovery. The ranges were limited so as to maintain the pressure mismatch between the primary and secondary nozzles at less than a factor of two. Increasing T_{0s} from 300 to 700K, R_L from 5 to 15, or ψ_s from 5 to 15, each resulted in about a 10% increase in the diffuser exit pressure. The increase in pressure recovery is due in part to the influence these parameters have on the cavity stagnation temperature ratio by increasing λ, e.g., see Eqs. (6) and (7), and in part to the way in which they alter the cavity inlet flowfield, M_3, P_3, etc.

Diffuser Experiments

A series of constant-area diffuser experiments were conducted with the following objectives: first, to provide a set of data for comparison with the analysis; second, to obtain data on the diffuser length/height ratio required to contain the shock system. The nozzle array used for these experiments was BCL-6, a two-dimensional array with nominal 1 × 4 in. envelope dimensions; it consisted of alternating fuel and oxidizer nozzles. The oxidizer nozzle had a geometric area ratio of 17; that of the fuel nozzle was 6. The laser cavity was 4 in. long, had an exit/inlet area ratio of 1.60, and water-cooled contoured walls to prevent boundary-layer separation. At the nozzle/cavity interface, the cavity wall divergence angle was 10°. The cavity was not equipped with optical apertures but rather had solid continuous sidewalls. The constant area diffuser section was 24 in. long and had a length/height ratio of 15. The subsonic diffuser was also 24 in. long, had an exit/inlet area ratio of 4.00, and 6° diverging walls. The cavity/diffuser assembly was 4 in. wide and had an overall length of 52 in. For all tests, the combustor fuel and oxidizer were H_2 and F_2, respectively; the combustor diluent was helium. Both H_2 and D_2 were used as cavity fuels; no diluent was added to the secondary flow, i.e., $\psi_s = 0$.

The tests were conducted in the following manner: with no laser flow, the system was evacuated to about 3 Torr using a three-stage steam-ejector system; laser flow was then established through the cavity diffuser exhausting to the 3-Torr facility back pressure; the pressure at the diffuser exit was then increased by injecting gaseous nitrogen into the exhaust duct downstream of the subsonic diffuser, moving the shock system into the diffuser until the pressure at the laser cavity exit just started to increase. When this occurred, the diffuser was operating against the maximum possible back pressure level that could be tolerated without disturbing the cavity flow, i.e., without moving shocks into the cavity. Once the shock system was stabilized, the cavity and diffuser pressure distributions were measured. Diffuser tests were conducted over the following range of test conditions: the combustor temperature (T_{02}) varied in the range of 1100-2100K, the combustor pressure (P_{02}) from 80 to 160 psia, combustor dilution level (ψ_p) from 16 to 45, and the cavity mixture ratio (R_L) from 5 to 15.

The cavity/diffuser pressure distribution for Test No. 531 is shown in Fig. 7. The laser cavity was instrumented with 12 pressure ports, the constant-area diffuser section with 31 ports, and the subsonic diffuser with 12 ports. The individual symbols shown in Fig. 7 each represent a single static pressure measurement; different symbols at the same axial location represent pressure measurements made on the top and sidewalls of the device, or at different transverse positions on the top wall. The solid line shown in Fig. 7 is a line drawn

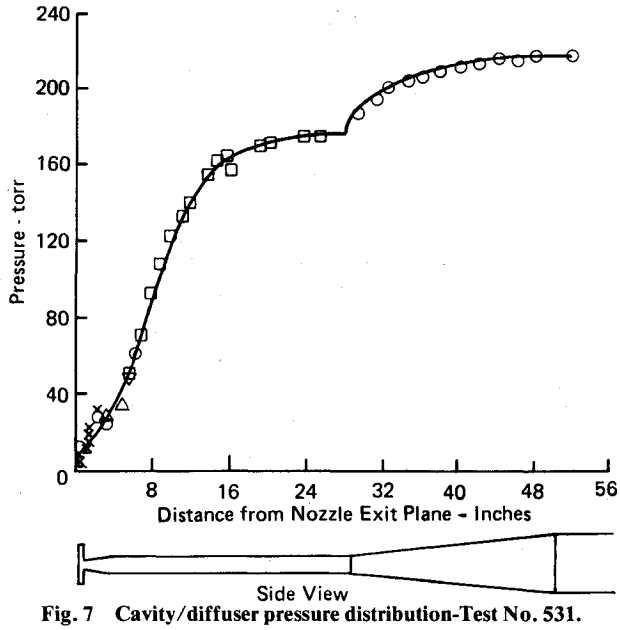

Fig. 7 Cavity/diffuser pressure distribution-Test No. 531.

through the pressure measurements to illustrate more clearly the pressure/distance characteristic.

For Test No. 531, the combustor pressure was 123 psia, the combustor temperature 1780K, and the flow dilution level was 19. The measured diffuser exit pressure was 218 Torr. For this test condition, the calculated value of the mixed average cavity inlet pressure is $P_3 = 16$ Torr, the measured wall pressure in the near-nozzle region shown in Fig. 7 is about 5 Torr. The difference between P_3 and the measured pressure is due to the Prandtl-Meyer expansion fan generated by the 10° cavity divergence angle at the nozzle/cavity interface. The wall pressure is measured downstream of the expansion fan and therefore is lower than P_3; indeed, an average cavity inlet pressure of 16 Torr yields a wall pressure of 4.5 Torr when the 10° expansion is taken into account. At the laser cavity exit (4 in. from the nozzle exit plane) the measured static pressure is about 30 Torr compared with a calculated value of 34 Torr; this twofold rise in the flow average static pressure across the laser cavity is due to the cavity combustion. Downstream of the cavity in the diffuser, the static pressure increases due to the shock and mixing phenomena that occur in the diffuser. The measured static pressure rise across the diffuser is 188 Torr, of which 145 Torr occurs in the constant-area section and 43 Torr in the subsonic diffuser; the importance of the subsonic diffuser is apparent since it contributes 23% of the overall diffuser static pressure rise. The analysis for this case yields a diffuser exit pressure of 217 Torr.

The constant-area diffuser section is 24 in. long and of the 145 Torr pressure rise that occurs in this section, 140 Torr occurs in the first 16 in. and only 5 Torr in the last 8 in. Thus, truncating this section at 16 in., yielding a 10/1 length/height ratio diffuser, would reduce the diffuser length by 33% with only a 3%, i.e., 5 Torr, decrease in performance. For the subsonic diffuser, if its length were reduced from 24 to 10 in., the pressure rise would be 35 Torr rather than 43 Torr. Taken together, the diffuser assembly length could be reduced by 18 in. (about 46%) with only a 13 Torr pressure recovery penalty.

Throughout these diffuser experiments, it was found that the constant area section length/height ratio required to contain the shock system increased as the diffuser inlet Mach number increased. For example, for the test data shown in Fig. 7, the diffuser inlet Mach number was calculated to be $M_4 = 2.20$, and the data indicates a required length/height ratio of approximately 10. In another test with $M_4 = 2.70$, the required ratio was about 15. These results are in agreement with the data trends presented by Neuman and Lustwenk,[14] although the required length appears to be somewhat greater

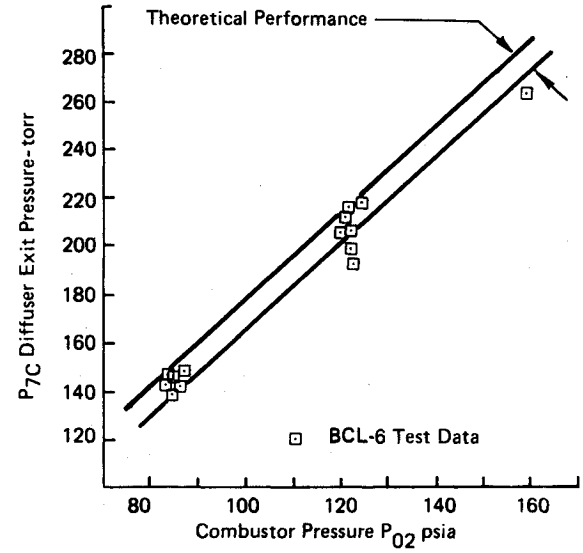

Fig. 8 BCL-6 diffuser data.

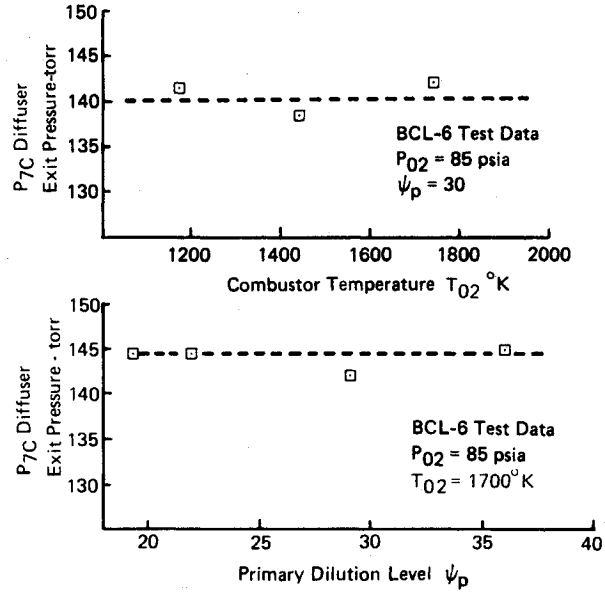

Fig. 9 Influence of combustor temperature and flow dilution on diffuser exit pressure.

in these laser experiments, possibly due to the low flow Reynolds numbers.

The diffuser exit pressures measured in 14 tests are shown in Fig. 8. The data indicates that the diffuser exit pressure increases approximately as a linear function of combustor pressure. Most of the test data falls within the theoretical performance band (band width ≈ 12 Torr) obtained from the analysis. Although the test conditions for the group of data clustered about the 85 psia combustor pressure covered a combustor temperature (T_{02}) range of 1100-1800K and a dilution level (ψ_p) range from 19-40, the diffuser exit pressures for these tests falls within a 10-Torr range. The results shown in Fig. 9 indicate that for these tests, the diffuser exit pressure is essentially independent of the combustor temperature and flow dilution level. This is in agreement with the theoretical results which indicate that the diffuser exit pressure is essentially invariant with changes in the flow chemistry when tests are conducted with a cavity of fixed area ratio and a constant area diffuser, e.g., Fig. 6. The conclusion drawn is that an increase in T_{02} or ψ_p must be coupled with a decrease in the cavity area ratio (A_4/A_3) in order to increase the diffuser exit pressure.

Conclusions

A one-dimensional flow model of the chemical laser was developed. The model encompasses the combustor, laser

nozzle array, cavity, and diffuser; in addition, real gas effects, nozzle and cavity boundary-layer losses, variable gas properties due to different fuel/oxidizer combinations, and the subsonic diffuser efficiency are included in the analysis. The analysis is in good agreement with diffuser data taken on a laser nozzle array operating with a constant area diffuser; it remains to verify the model with second throat diffuser data.

The analysis indicates that the diffuser inlet Mach number is generally less than 3.00, and about 2.30 for the nominal conditions of this study; in this Mach number range, a second throat diffuser could potentially increase the diffuser exit pressure by about 20%. In terms of the flow variables, the combustor temperature has the greatest effect on pressure recovery; increasing T_{02} from a nominal 1700 to 2100K can yield about a 25% increase in the diffuser exit pressure. With a constant-area diffuser, diluent placement did not appear to be critical, e.g., increasing ψ_s from 5 to 15 or ψ_p from 25 to 35 both yielded about a 12% increase in pressure recovery; with a second throat diffuser, it was found to be more effective to place diluent in the primary rather than the secondary stream. Increasing the secondary stream stagnation temperature, T_{0s}, from a nominal 300-700K resulted in about a 10% improvement in the diffuser exit pressure.

Both the analysis and experiment show the importance of being able to vary the laser cavity area ratio as the cavity inlet flow conditions are changed. In pressure recovery experiments, the cavity-area ratio should be considered as a primary variable. Measured diffuser exit pressures were found to be a linearly increasing function of the combustor pressure; this is in agreement with the analaysis that indicates the slope and intercept of this characteristic line are dependent on the nozzle design features and the laser cavity area ratio. Of the diffuser pressure rise, 20% was measured to occur in the subsonic diffuser, the remainder in the constant area section. The length to height ratio of the constant area section required to convert the flow from supersonic to subsonic velocities was found to be dependent on the diffuser inlet conditions; the experimental results indicate length/height ratios of 10-15 are required.

Appendix

The primary and secondary flows mix and react in a constant-area cavity. At the cavity exit (station 4), the flow is uniform and the reactions complete; the stagnation temperature and molecular weight at this location are T_{04} and M_{w4}. Assume the primary, secondary, and cavity exit flow have the same specific heat ratio for simplicity. Neglecting the base pressure term, which is small, the momentum equation is given by

$$[PA(1+\gamma M^2)]_4 = [PA(1+\gamma M^2)]_p + [PA(1+\gamma M^2)]_s \quad \text{(A1)}$$

Write the continuity equation as

$$\frac{m(RT_0)^{1/2}}{PA} = M\left[\gamma\left(1+\frac{\gamma-1}{2}M^2\right)\right]^{1/2} \quad \text{(A2)}$$

if Eq. (A2) is solved for PA and substituted into each of the three terms in Eq. (A1), then the solution for M_4 can be written

$$F(\gamma,M_4) = Y_p\left[\frac{T_{0p}M_{w4}}{T_{04}M_{wp}}\right]^{1/2}F(\gamma,M_p) + Y_s\left[\frac{T_{0S}}{T_{04}}\frac{M_{w4}}{M_{wS}}\right]^{1/2}F(\gamma,M_S) \quad \text{(A3)}$$

where the Mach number function $F(\gamma,M)$ is defined by

$$F(\gamma,M) = (1+\gamma M^2)M^{-1}\left[\gamma\left(1+\frac{\gamma-1}{2}M^2\right)\right]^{-1/2} \quad \text{(A4)}$$

The mixing and heating process is now separated into two distinct steps. The primary and secondary flows enter the cavity and are fully mixed at station 3 where the stagnation temperature and molecular weight are T_{03} and M_{w3}. Between stations 3 and 4, the chemical reactions occur, and the gas is heated. The flow Mach number at station 3 is given by

$$F(\gamma,M_3) = Y_p\left[\frac{T_{0p}M_{w3}}{T_{03}M_{wp}}\right]^{1/2}F(\gamma,M_p) + Y_S\left[\frac{T_{0S}M_{w3}}{T_{03}M_{wS}}\right]^{1/2}F(\gamma,M_S) \quad \text{(A5)}$$

which is Eq. (A3) with T_{03} and M_{w3} substituted for T_{04} and M_{w4}. For the heating process, M_3 and M_4 are related by

$$F(\gamma,M_4) = \left[\frac{T_{03}M_{w4}}{T_{04}M_{w3}}\right]^{1/2}F(\gamma,M_3) \quad \text{(A6)}$$

If Eq. (A5) is substituted into Eq. (A6), then Eq. (A3) results, indicating that for constant-area flows, the calculation for M_4 is independent of the path taken to describe the mixing and reaction processes. A similar result can be shown for a constant-pressure cavity.

References

[1]Warren, W. R., "Chemical Lasers," *Astronautics and Aeronautics*, Vol. 13, April 1975, pp. 36-49.

[2]Mirels, H., Hofland, R., and King, W. S., "Simplified Model of CW Diffusion-Type Chemical Laser," *AIAA Journal*, Vol. 11, Feb. 1973, pp. 156-164.

[3]Warren, W. R., "Reacting Flow and Pressure Recovery Processes in HF/DF Chemical Lasers," The Aerospace Corp., El Segundo, Calif., TR-0074 (9240-02)-1, Nov. 1973.

[4]Durran, D. A. and Liu, S. W., "Pressure Recovery in a Constant Area Diffuser for Chemical Lasers with Nozzle Base Relief," The Aerospace Corp., El Segundo, Calif., SAMSO-TR-75-147, June 1975.

[5]Ferri, A., "Review of SCRAMJET Propulsion Technology," *Journal of Aircraft*, Vol. 5, Jan. 1968, pp. 3-10.

[6]Ferri, A. and Fox, H., "Analysis of Fluid Dynamics of Supersonic Combustion Process Controlled by Mixing," *Twelfth Symposium (International) on Combustion*, The Combustion Institute, Pittsburgh, Pa., 1969, pp. 1105-1113.

[7]Billig, F. S., "Design of Supersonic Combustors Based on Pressure-Area Fields," *Eleventh Symposium (International) on Combustion*, The Combustion Institute, Pittsburgh, Pa., 1967, pp. 755-769.

[8]Billig, F. S. and Dugger, G. L., "The Interaction of Shock Waves and Heat Addition in the Design of Supersonic Combustors," *Twelfth Symposium (International) on Combustion*, The Combustion Institute, Pittsburgh, Pa., 1969, pp. 1125-1139.

[9]Billig, F. S., Orth, R. C., and Lasky, M., "Effects of Thermal Compression on the Performance Estimates of Hypersonic Ramjets," *Journal of Spacecraft and Rockets*, Vol. 5, Sept. 1968, pp. 1076-1081.

[10]Cookson, R. A., Flanagan, P. and Penny, G. S., "A Study of Free-Jet and Enclosed Supersonic Diffuser Flames," *Twelfth Symposium (International) on Combustion*, The Combustion Institute, Pittsburgh, Pa., 1969, pp. 1115-1124.

[11]Crocco, L., One-Dimensional Treatment of Steady Gas Dynamics, *Fundamentals of Gas Dynamics*, Vol. III, Princeton University Press, Princeton, N.J., 1958.

[12]Driscoll, R. J., "A Study of the Boundary Layers in Chemical Laser Nozzles," *AIAA Journal*, Vol. 14, Nov. 1976, pp. 1571-1577.

[13]Zelazny, S. W. and Rushmore, W. L., "The Effect of Mixing Rate on Pressure Fields in Confined Flows," AIAA Paper 77-221, Washington, D.C., 1977; submitted to *AIAA Journal*.

[14]Neuman, E. P. and Lustwerk, F., "Supersonic Diffusers for Wind Tunnels," *Journal of Applied Mechanics*, Vol. 16, June 1949, pp. 195-202.

[15]Shapiro, A. H., *The Dynamics and Thermodynamics of Compressible Fluid Flow*, Vol. I, Ronald Press, New York, 1953, Chap. 5.

[16]Rundstandler, P. W. and Dean, R. C., "Straight Channel Diffuser Performance at High Inlet Mach Numbers," *Transactions of the ASME, Journal of Basic Engineering*, Sept. 1969, pp. 397-422.

[17]Hasel, L. E. and Sinclair, A. R., "A Preliminary Investigation of Methods for Improving the Pressure Recovery Characteristics of Variable Geometry Supersonic Subsonic Diffuser Systems," NACA-RM-L57H02, Oct. 1957.

[18]Neuman, E. P. and Lustwerk, F., "High Efficiency Supersonic Diffusers," *Journal of the Aeronautical Sciences*, Vol. 18, June 1951, pp. 369-374.

[19]Panesci, J. H. and German, R. C., "An Analysis of Second Throat Diffuser Performance for Zero Secondary Flow Ejector Systems," Arnold Engineering Development Center, Tullahoma, Tenn., TDR-63-249, Dec. 1963.

[20]Wilson, L. E. and Hook, D. L., "Deuterium Flouride CW Chemical Lasers," AIAA Paper 76-344, San Diego, Calif., 1976.